THE JOURNAL OF BIOLOGICAL CHEMISTRY VOL. 284, NO. 16, pp. 10783–10792, April 17, 2009

Investigation of Fatty Acid Elongation and Desaturation Steps in *Fusarium lateritium* by Quantitative Two-dimensional Deuterium NMR Spectroscopy in Chiral Oriented Media[S]

Received for publication, October 10, 2008, and in revised form, February 11, 2009 Published, JBC Papers in Press, February 12, 2009, DOI 10.1074/jbc.M807826200

Vincent Baillif[‡], Richard J. Robins[‡], Steven Le Feunteun[‡], Philippe Lesot[§], and Isabelle Billault[‡1]

From the [‡]Université de Nantes, CNRS, UFR des Sciences et Techniques, Chimie et Interdisciplinarité Synthèse, Analyse, Modélisation, UMR CNRS 6230, 2 Rue de la Houssiniere, BP 92208 44322 Nantes Cedex 3 and the [§]Université de Paris Sud (11), ICMMO, UMR CNRS 8182, Laboratoire de Structurale Organique, RMN en Milieu Orienté, 91405 Orsay, France

The origin of hydrogen atoms during fatty acid biosynthesis in *Fusarium lateritium* has been quantified by isotope tracking close to natural abundance. Methyl linoleate was isolated from *F. lateritium* grown in natural abundance medium or in medium slightly enriched with labeled water, glucose, or acetate, and the ^2H incorporation was determined by quantitative ^2H-{^1H} NMR in isotropic and chiral oriented solvents. Thus, the individual $(^2H/^1H)_i$ ratio at each pro-*R* and pro-*S* hydrogen position of the CH_2 groups along the chain can be analyzed. These values allow the isotope redistribution coefficients (a_{ij}) that characterize the specific source of each hydrogen atom to be related to the nonexchangeable hydrogen atoms in glucose and to the medium water. In turn, these can be related to the stereoselectivity that operates during the introduction or removal of hydrogens along the fatty acid chain. First, at even CH_2 the pro-*S* hydrogen comes only from water by protonation, whereas the pro-*R* hydrogen is introduced partly via acetate but principally from water. Second, the nonexchangeable hydrogens of glucose (positions H-6,6 and H-1) are shown to be introduced to the odd CH_2 via the NAD(P)H pool used by both reductases involved in the elongation steps of the fatty acid chain. Third, it is proved that hydrogens removed at sites 9,10 and 12,13 during desaturation by Δ^9- and Δ^{12}-desaturases are pro-*R*, and that during these desaturation steps α-secondary kinetic isotope effects occur at the 9 and 12 positions and not at the 10 and 13 positions.

Fatty acids are ubiquitous natural products involved in many key biological processes, including acting as components of membranes, as lipophilic modifiers, as fuel stores, and as precursors of intracellular messengers (1–3). Their biosynthesis, which is strictly conserved throughout higher organisms, can be separated into two parts as follows: the formation of the basic C16 unit, palmitoyl-CoA (C16:1), by the fatty-acid synthase complex (FAS)[2] and the subsequent modification of this chain by a range of elongases, desaturases, conjugases, hydroxylases, and epoxidases. Many of these steps involve stereoselective enzymatic reactions during which hydrogen atoms are inserted or eliminated.

We have previously shown that this process leads to a distribution of ^2H in long chain fatty acids that is nonstatistical (4–7). Thus, isotopic fractionation is seen to be introduced. Two features general to all organisms so far examined can be noted. First, the methylenic groups at even positions tend to be richer than those at odd positions. Second, one of the ethylenic groups present at the positions of desaturation is consistently impoverished relative to the methylenic sites, whereas the other is not.

Thus, each hydrogen atom in the final product will have a ($^2H/^1H$) ratio that is representative of its initial origin, its passage through the FAS elongation steps, and its potential participation in post-elongation modification of the chain. To date, it has proved possible to explain part of the observed ($^2H/^1H$) ratios on the basis of the described mechanisms and measured isotope effects of the enzymes involved in these reactions. In this way, it has been shown that the hydrogens at odd positions are essentially derived from NAD(P)H (8, 9), whereas those at even positions are derived in a very variable ratio from acetate and water (10–12) (Fig. 1). Similarly, it has been demonstrated that it is the pro-*S* position that is retained during desaturation (12–14). However, to understand the relative impact of these different causes on the observed distribution patterns of ^2H in natural fatty acids, it is necessary to define the quantitative links between different hydrogen positions in the fatty acid and those in the carbohydrate substrates or water from which these have been introduced. Only then will it be possible to elucidate the relative importance of each of the characteristics that have been individually described, *i.e.* substrate, hydrogen elimination reactions, and hydrogen addition reactions, in defining the ($^2H/^1H$) ratios observed in the final product.

The distribution pattern of ^2H in a product can be accessed directly by quantitative ^2H-{^1H} NMR in isotropic media at natural abundance or at a level of enrichment in ^2H too low to induce any significant isotope effect (typically 2–5-fold is used). The links between these values measured in the product and those for the various available origins of hydrogen can then be quantified using a simple linear model, which describes the amount of hydrogen at each position derived from water and

[S] The on-line version of this article (available at http://www.jbc.org) contains supplemental Figs. SD1–SD4 and Table SD1.

[1] To whom correspondence should be addressed: Elucidation of Biosynthesis by Isotopic Spectrometry Group, Bât 9, CEISAM, UMR CNRS6230, University of Nantes, 2 Rue de la Houssinière, BP 92208, 44322 Nantes Cedex 3, France. Tel.: 332-5112-5709; Fax: 332-5112-5712; E-mail: isabelle.billault@univ-nantes.fr.

[2] The abbreviations used are: FAS, fatty-acid synthase; PBLG, poly-γ-benzyl-L-glutamate; KIE, kinetic isotope effect; FAME, fatty acid methyl ester.

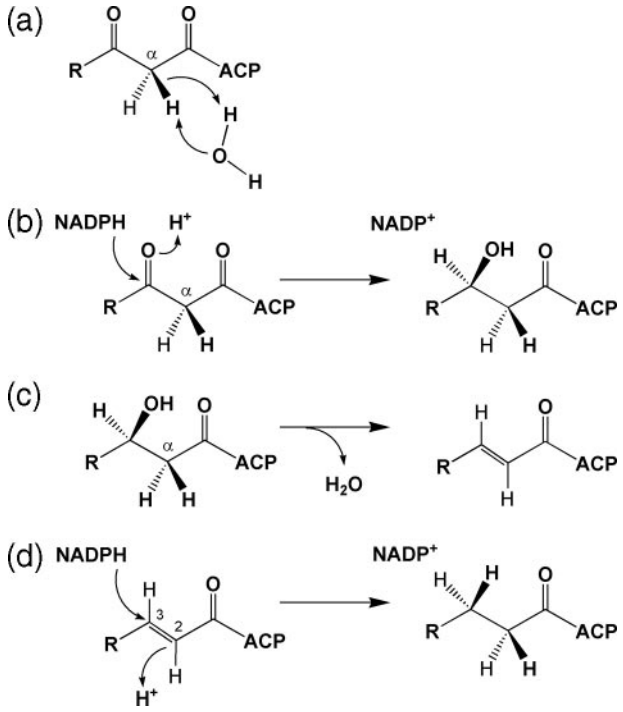

FIGURE 1. **Different steps during which hydrogen is added or eliminated during fatty acid biosynthesis.** *a,* post-malonate exchange, retention of pro-*S* > pro-*R*; *b,* FAS, β-ketoacyl reductase, *si* face attack; *c,* FAS, β-hydroxybutyryl-ACP dehydratase, *syn* dehydration with elimination of α pro-*S* hydrogen; *d,* FAS, enoyl reductase, 2*si*-3*si* attack in *S. cerevisiae* and 2*si* face in fungi.

from each position in the substrate. Hence, the site-specific isotopic ratio at position *i* of a product, $(^2H/^1H)_i$, can be defined by Equation 1 (15–19),

$$(^2H/^1H)_i = a_{im}(^2H/^1H)_m + \sum_j a_{ij}(^2H/^1H)_j \qquad \text{(Eq. 1)}$$

where $(^2H/^1H)_m$ is the isotopic ratio of the medium and $(^2H/^1H)_j$ is the isotopic ratio at a given site *j* of the substrate. The terms a_{im} and a_{ij} are the isotope redistribution coefficients that furnish the quantitative description of these links, reflecting both the quantity of hydrogen transferred from a given origin and the associated kinetic isotope effects (KIEs) for a defined set of biochemical reactions (20, 21). Clearly, for some hydrogen positions *j* in the substrate, $a_{ij} = 0$.

Analysis of long chain fatty acids by ^2H-{^1H} one-dimensional NMR in isotropic media is inadequate for the description of isotope redistribution coefficients since: (i) not all methylenic and ethylenic sites are resolved, and (ii) none of the large number of enantiotopic pro-*R*/*S* sites present can be observed (4, 6, 7, 21, 22). Such resolution is essential in interpreting hydrogen-atom origin, particularly in view of the domination of fatty acid biosynthesis by a series of enantioselective reactions (Fig. 1).

Recently, it has been shown that the application to fatty acids of two-dimensional ^2H NMR in solutes embedded in polypeptide chiral liquid crystals effectively overcomes the lack of spectral resolution in isotropic one-dimensional ^2H-{^1H} NMR, offering both access to the majority of methylenic and ethylenic sites and the resolution of pro-*R* and pro-*S* enantiotopic hydrogens (23–25). This has opened the way to an in-depth measurement of the natural ^2H distribution at the pro-*R*/*S* sites of fatty

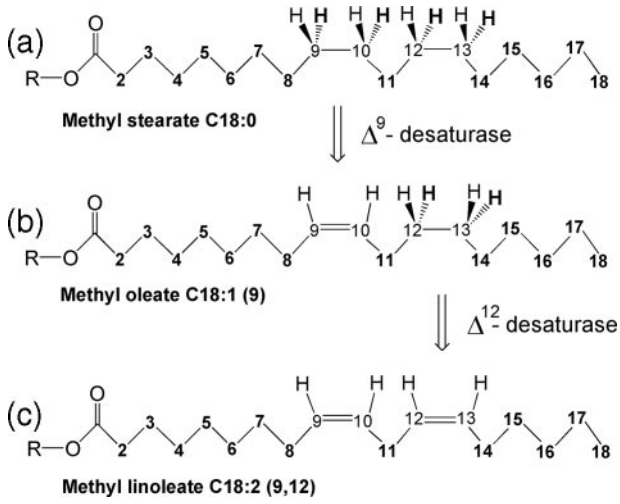

FIGURE 2. **Desaturation steps performed by the Δ^9- and Δ^{12}-desaturases on methyl stearate (*a*) and methyl oleate (*b*), respectively, leading to methyl linoleate (*c*).** Hydrogen atoms in *boldface* are at pro-*R* positions (R = CH_3).

acids produced *in vivo* from defined substrates at sufficient resolution to relate the observed values to the interplay *in vivo* between the causes of variation.

To provide adequate amounts of fatty acids for ^2H NMR analysis under strictly defined environmental conditions, we have exploited the oleaginous filamentous fungus *Fusarium lateritium,* which accumulates fatty acids under conditions of carbon excess (26). These include ~25% linoleic acid (C18:2; 9,22), a particularly pertinent target for this study as it is a key precursor from which numerous other fatty acids are biosynthesized (27). Thus, cultures can be grown in controlled media on site-specifically slightly ^2H-enriched glucose, slightly enriched water, or slightly enriched sodium acetate and the ^2H incorporation into different positions of linoleic acid ascertained. Consequently, in contrast to previous studies on fatty acids extracted from natural sources, the relationship between substrate and the $(^2H/^1H)$ ratios observed can be obtained under directly comparable conditions.

Hence, for the first time, the ^2H linkage between a large number of hydrogen atoms in linoleic acid and its precursors *in vivo* can be quantitatively tested and related to the stereospecificity of the reductases in the FAS complex, hydrogen exchange reactions in the reduced nucleotide (NAD(P)H) pools (10), "post-malonate" exchange (11), the stereospecificity of hydrogen abstraction in the Δ^9- and Δ^{12}-desaturation steps (Fig. 2), and the KIEs associated with these reactions.

EXPERIMENTAL PROCEDURES

Materials—D-(+)-Glucose (Rectapur grade) at natural abundance was purchased from Prolabo. Specifically labeled [1-^2H]glucose, [6,6-$^2H_2$]glucose (both 98 atom %), and ([2-$^2H_3$]acetate·Na) (99.4 atom %) were obtained from EurisoTop. ^2H_2O (99.9 atom %) was obtained from Sigma. Poly-γ-benzyl-L-glutamate (PBLG) used for anisotropic NMR with a degree of polymerization of 782 (M_r ≈171,300) was from Sigma.

Fungal Cultures—The filamentous fungus *F. lateritium* was kindly supplied by Professor C. Ratledge, Department of Bio-

logical Sciences, University of Hull, UK. The fungus was maintained on Potato Dextrose Agar (39 g/liter) (Biokar). Culture was transferred to fresh plates every 3 weeks and grown at 27 °C for 72 h before storage at 4 °C.

General Methods—Solvents for liquid chromatography were distilled before use. Chloroform (stabilized with ethanol), used for the preparation of NMR samples in chiral oriented media, was dried using molecular sieves.

Growth Medium at Natural Abundance—The basal medium used contained the following per liter of distilled water: KH_2PO_4, 7 g; $Na_2HPO_4{\cdot}12H_2O$, 3.33 g; $MgSO_4{\cdot}7H_2O$, 2.16 g; yeast extract, 1.5 g; L-tartaric acid, 1.2 g; NH_4Cl, 0.86 g; $CaCl_2{\cdot}2H_2O$, 0.12 g; $FeCl_3{\cdot}6H_2O$, 9 mg; $ZnSO_4{\cdot}7H_2O$, 1.9 mg. The carbon source used was glucose (40 g/liter). To prevent foaming, PEG 5000 (2.5 g/liter) (Sigma) was added. The pH was adjusted to 5.5 with NaOH (2.5 M).

Growth Medium at Slight Enrichment—Glucose samples slightly enriched were prepared by adding small amounts (~40 mg) of the corresponding deuterated glucose to a solution of the reference glucose (120 g) dissolved in 3 liters of Nantes tap water. The $(^2H/^1H)_j$ of reference glucose was measured as described in Ref. 28, and the final $(^2H/^1H)_i$ was calculated as described previously (16, 17). Water slightly enriched in ^2H was prepared by adding ^2H_2O (0.2 ml/liter) to Nantes tap water (3 liters). The $(^2H/^1H)_m$ ratios of both the Nantes tap water and the slightly enriched water were determined by ^2H NMR. The $(^2H/^1H)_j$ ratios of substrates at natural abundance and of the slightly enriched substrates present in the different culture media (A–E) are given in Table 1.

Fermentation Conditions—Cultures (3 liters) were grown in a 6-liter round-bottomed fermentation vessel. Incoming and outgoing air was passed through 0.2-μm filters (Midisart® 2000). The assembled vessel containing 3 liters of medium was sterilized by autoclaving at 121 °C for 30 min. For inoculum, an ~10-mm square was cut from an 8–12-day-old *F. lateritium* stock culture plate and shaken with ~30 ml medium in an inoculum bottle containing quartz chips. After settling, the liquid phase was added aseptically to the fermentor. The vessel was placed in an incubator at 28 °C, the airflow rate was set at 2 liters/min, and the culture was stirred at 500 rpm for 7–9 days. Glucose (40 g in 200 ml medium), with the same isotopic signature as that used in the starting medium, was added at days 5 and 7. Culture growth (wet biomass/volume) and fatty acid production were followed in an aliquot (100 ml) taken as appropriate. When dry biomass reached ~30 g/liter (8–9 days), the culture was stopped. Cells were recovered from the medium by filtration on a Buchner funnel through nylon mesh, washed with distilled water, centrifuged (4250 × *g*; 10 min), fast-frozen in liquid N_2, and freeze-dried.

Fatty Acid Methyl Ester (FAME) Extraction and Methyl Linoleate Isolation—Direct transesterification was used to extract the FAMEs from the dry biomass. To a fresh solution of NaOH in MeOH (50 g in 200 ml) was added 25 g of crushed freeze-dried cells. The mixture was heated under reflux for 30 min, cooled to room temperature, and a solution of BF_3-MeOH (50%; 90 ml) added dropwise. The reaction mixture was again heated under reflux for a further 45 min and then cooled to room temperature. After filtration on a Buchner funnel (Whatman No. 1), the filtrate was diluted with cyclohexane (300 ml) and transferred to a separating funnel containing saturated brine (300 ml). The aqueous layer was extracted with cyclohexane (three times 150 ml), and the organic phases were pooled, washed with water, dried over $MgSO_4$, and evaporated to afford FAMEs as a yellow oil (5.7–8.9 g). Methyl linoleate was isolated from the FAME mixture by chromatography on silica gel impregnated by silver nitrate as described previously (4).

Quantification of FAME Mixtures—The composition of FAME extracts was analyzed by gas chromatography on an HP6890 series II gas chromatograph with an SPB™-PUFA capillary column (30 m × 0.32 mm, film thickness 0.52 μm; Supelco); carrier gas, helium, 1.2 ml/min (constant flow); split 1:40; injector temperature, 250 °C; flame ionization detector temperature, 280 °C. Elution conditions were as follows: 140 °C for 2 min, ramped at 8 °C/min to 210 °C, 210 °C for 25 min. Identification of fatty acid methyl esters was based on the comparison of retention times with known standards. The fatty acid compositions were expressed as a percentage of the sum of the peak areas.

Deuterium NMR Spectroscopy—All ^2H-{^1H} NMR spectra (in liquid and chiral oriented media) were recorded on a Bruker Avance II 600 MHz NMR spectrometer (14.1 tesla) equipped with a 5-mm selective ^2H cryogenic probe (92.1 MHz) operating without a ^{19}F lock device. The WALTZ-16 sequence was applied to decouple protons. The temperature of all NMR tubes was regulated carefully at 310 K for the liquid media experiments and at 300 K for the chiral oriented media.

Samples were prepared as follows: (*a*) for liquid media experiments, methyl linoleate (0.15 g), the isotopic reference, pyridine (0.07 g), and solvent $CHCl_3/CCl_4$ (1:4.5; 2.1 g) were mixed and then filtered and transferred into a 5-mm NMR tube; (*b*) for chiral oriented media, the standard procedure to prepare samples using 5-mm NMR tubes was as described in previous papers (24, 29, 30). In this study, all PBLG/$CHCl_3$ samples were prepared by dissolving 100 ± 1 mg of methyl linoleate in 100 ± 1 mg of PBLG and 650 ± 1 mg of dry $CHCl_3$. To reach the best spectral resolution, several cycles of centrifugation and re-homogenization of the sample were carried out to remove concentration gradients. NMR tubes were fire-sealed to avoid solvent evaporation. ^2H-{^1H} one-dimensional NMR acquisition conditions are described below. Three replicate acquisitions were carried out for each sample and each condition (*a* and *b*).

Condition a, Liquid Media Experiments—NMR spectra were recorded in quantitative conditions with a repetition time greater than (5-fold), the longest relaxation time (T_1), and a flip angle of 90°. Sampling period (AQ) was as follows: 3.5 s; repetition time (T_R), 5.7 s; number of scans (*NS*), 3200. An exponential filtering (LB) of 1 Hz was applied. An example of an isotropic quantitative ^2H one-dimensional NMR spectrum of methyl linoleate is shown in supplemental Fig. SD1.

Condition b, Two-dimensional Experiments in Chiral Oriented Media—The phased ^2H-{^1H} two-dimensional NMR spectra were recorded using the *Q*-COSY Fz sequence. The value of these two-dimensional experiments is the direct autocorrelation of the two components of each quadrupolar doublet to simplify the analysis of overcrowded deuterium one-dimensional spectra (24, 30, 31). A scheme illustrating the two-di-

TABLE 1
$(^2H/^1H)_i$ ratios (in ppm) of labeled substrates used in cultures A–E

Culture	Culture conditions	$(^2H/^1H)_{H_2O}$	$(^2H/^1H)_{Glc\text{-}6,6}$	$(^2H/^1H)_{Glc\text{-}1}$	Mass [2-$^2H_3$]acetate·Na
					mg/liter
A	NA[a]	148.9	148.9	168.2	
B	^2H_2O	318.1	148.9	168.2	
C	[6,6-$^2H_2$]Glucose	148.9	481.6	168.2	
D	[1-^{2}H]Glucose	148.9	148.9	663.5	
E	[2-$^2H_3$]Acetate·Na[b]	148.9	148.9	168.2	110.0

[a] NA means natural abundance level in ^{2}H.
[b] [2-$^2H_3$]Acetate·Na indicates enriched in deuterium at 99.4 atom %.

TABLE 2
Composition of the FAMEs extracted from cultures A–E

Culture	Culture conditions	Biomass[a]	FAME[b]	FAME (%/biomass)	Fatty acid methyl ester			
					C16:0	C18:0	C18:1(9)	C18:2(9,12)
		g/liter	*g*		*%*	*%*	*%*	*%*
A	NA[c]	22.3	8.4	33.4	29.1	4.1	41.8	21.6
B	^2H_2O	20.4	5.8	24.0	31.2	4.9	38.4	23.1
C	[6,6-$^2H_2$]Glucose	18.0	5.7	23.0	28.9	3.1	34.2	29.8
D	[1-^{2}H]Glucose	18.6	7.6	30.5	29.9	3.7	41.3	22.6
E	[2-$^2H_3$]Acetate·Na	16.1	8.9	35.7	28.2	3.9	43.8	18.2
Mean		19.1	7.1	29.3	29.5	3.9	39.9	23.0
S.D.		2.4	1.8	5.6	1.1	0.6	3.7	4.2

[a] Dry biomass is meant.
[b] Mass of FAMEs was obtained from 25 g of dry biomass.
[c] NA means natural abundance level in ^{2}H.

mensional NMR pulse sequence is given in supplemental Fig. SD2, and the associated theory is discussed in Ref. 31. In practice, 96 FIDs for each t_1 increment and a two-dimensional matrix of 1530 (t_2) × 512 (t_1) data points were used, and the same spectral width (1700 Hz) was chosen in both dimensions. The recycling time for each scan was 1 s (27), leading to a total acquisition time of around 15 h. Exponential filtering (LB) of 1–1.5 Hz was applied in both dimensions. The two-dimensional experiments were zero-filled to 2048 (t_1) × 2048 (t_2) data points prior to two-dimensional Fourier transformation, and then symmetrized and tilted. An example of an anisotropic ^{2}H two-dimensional NMR spectrum of methyl linoleate (resulting from culture D) is given in supplemental Fig. SD3. The quantitative measurement of the areas under the peaks of the ^{2}H NMR signals was performed using a curve-fitting algorithm of a complex least squares treatment (PERCH solutions Ltd., Kuopo, Finland), and the site-specific $(^2H/^1H)_i^{iso}$ ratios (expressed in parts per million) were calculated as described previously (32).

The $(^2H/^1H)_i^{aniso}$ at all CH_2 and some resolved pro-*R*/*S* sites of methyl linoleate were calculated from both sets of data as follows: the area percentage of quadrupolar doublets detected at the same chemical shift on the two-dimensional map of *Q*-COSY experiment and the $(^2H/^1H)_i^{iso}$ ratios determined by isotropic NMR using Equation 2 (24, 33),

$$\left(\frac{^2H}{^1H}\right)_i^{aniso} = \left(\frac{(\%area)}{100} \times n \times \left(\frac{^2H}{^1H}\right)_i^{iso}\right) \qquad \text{(Eq. 2)}$$

where n is the number of ^{2}H sites with a coincident chemical shift contributing to the ^{2}H NMR signal recorded in liquid medium.

RESULTS

Culture of F. lateritium and Isolation of Methyl Linoleate—Fatty acids were extracted as their methyl esters from cultures of the oleaginous filamentous fungus *F. lateritium* grown in media supplemented with different slightly enriched sources of ^{2}H: water, glucose, or acetate (Table 1, cultures B–E). The reference culture was grown in natural abundance water and glucose (Table 1, culture A). The growth and fatty acid production are given in Table 2.

Methyl linoleate purified from each culture was recovered at ~95% yield; 0.6–1.6 g was isolated depending on the mass and % composition of the starting mixture. The purity was confirmed by gas chromatography to be >95% in all cases.

Determination of $(^2H/^1H)$ Ratios of Methyl Linoleate by Quantitative ^2H NMR in Liquid and Chiral Oriented Media—The *Q*-COSY Fz map recorded in the chiral liquid crystal mesophase shows that numerous ^{2}H sites that had coincident resonances in the isotropic ^{2}H-{^{1}H} NMR spectrum are clearly separated on the basis of a quadrupolar splitting difference (supplemental Fig. SD3). We have previously reported and justified the assignment of all quadrupolar doublets to each methylene group and the *R*/*S* stereochemical attribution of doublets corresponding to methylene sites showing an enantiodiscrimination (see supplemental Fig. SD4) (24). The principle on which these assignments are made is explained in the supplemental material.

For each methyl linoleate isolated from cultures A–E, ^{2}H-{^{1}H} NMR spectra in both liquid and chiral oriented media were recorded following quantitative acquisition conditions as described previously (24). The $(^2H/^1H)_i^{iso}$ ratios determined in liquid media for CH_2 sites 2–18 are given in supplemental Table SD1.

As sample composition and spectral acquisition conditions were identical to those used in Ref. 24, the relative position of quadrupolar doublets (centered on the same chemical shift) in the ^{2}H *Q*-COSY Fz two-dimensional NMR spectra were the same, making it possible to assign the stereochemistry of each

TABLE 3
$(^2H/^1H)_i^{aniso}$ ratios (in ppm) for methyl linoleate extracted from cultures A to E measured by ^2H NMR in liquid and chiral oriented media

Culture	Site	2[c]		3[c]		4	5	6	7	8[c]		9	10	11	12	13	14[c]		15[c]		16,17	18
		pro-R	pro-S	pro-R	pro-S	CH_2	CH_2	CH_2	CH_2	pro-R	pro-S	C=CH	C=CH	CH_2	C=CH	C=CH	pro- R	pro-S	pro-R	pro-S	$2CH_2$	CH_3
NA A	$(^2H/^1H)_i^{aniso\ a}$	121.4	125.2	134.1	90.4	110.9	121.3	127.1	116.4	107.0	104.9	59.4	139.8	110.8	105.2	106.8	131.7	122.9	221.8	87.9	97.4	119.2
	S.D.	3.1	3.1	1.8	1.8	2.6	3.2	4.6	5.1	5.5	7.5	2.5	4.2	2.4	2.3	4.9	3.1	1.9	7.4	5.6	1.0	1.8
^2H_2O B	$(^2H/^1H)_i^{aniso\ a}$	251.0	275.4	189.9	122.1	240.3	180.7	279.8	174.7	204.6	222.5	83.9	295.8	172.0	237.6	157.9	269.6	274.6	355.6	144.9	197.4	219.2
	S.D.	1.0	1.0	8.6	8.6	7.2	12.1	15.5	10.1	5.0	13.1	9.1	4.9	0.1	4.5	5.1	11.4	11.5	5.1	6.3	6.7	0.3
[6,6-$^2H_2$]glucose C	$(^2H/^1H)_i^{aniso\ a}$	143.9	135.9	140.4	86.2	128.9	129.1	153.4	126.4	122.6	98.9	47.8	139.6	108.7	101.5	95.5	173.8	124.9	268.0	91.9	105.6	191.4
	S.D.	6.0	6.0	5.5	5.5	9.4	0.8	1.3	7.8	5.2	3.3	5.6	3.3	0.8	7.3	2.2	6.4	1.6	10.1	8.9	12.1	07
[1-^2H]glucose D	$(^2H/^1H)_i^{aniso\ a}$	130.5	127.7	187.6	113.2	115.5	158.9	125.3	157.7	108.6	101.7	73.3	136.2	139.2	93.5	131.5	141.9	122.6	312.0	118.3	120.2	142.93
	S.D	5.0	5.0	6.8	6.8	2.0	9.7	3.4	2.0	4.0	5.5	6.2	8.1	1.4	2.8	1.3	5.0	4.9	18.9	3.6	2.1	0.5
[2-$^2H_3$]acetate.Na E	$(^2H/^1H)_i^{aniso\ b}$	1113.9	376.9	188.6	134.5	846.8	115.3	811.6	79.7	1587.5	89.7	67.7	184.8	145.6	136.2	132.1	2229.5	128.3	248.0	88.6	687.7	2987.8

[a] $(^2H/^1H)_i^{aniso}$ values were calculated from three ^2H NMR spectral acquisitions recorded in chiral oriented media and liquid media (see supplemental Table SD2 for $(^2H/^1H)_i^{iso}$ ratios from ^2H NMR spectra in liquid media). S.D., standard deviation.
[b] $(^2H/^1H)_i^{aniso}$ values were calculated from one ^2H NMR spectral acquisition.
[c] The attribution to pro-*R* and pro-*S* positions is based on previous work; for site 8, this attribution should be reversed if CIP rules are applied rather than the origin of hydrogen (24).

quadrupolar doublet to the *R* and *S* enantioisotopomers (as shown in supplemental Fig. SD4). The $(^2H/^1H)_i$ ratios thus determined for CH_2 sites 2–18 are presented in Table 3. The standard deviation values in Table 3 were calculated from three different acquisitions and were found acceptable, mostly less than 5 ppm (<5%) except for a few higher values for some $(^2H/^1H)_i^{aniso}$ ratios, which are still <8%.

Thus, by combining the ^2H NMR data from liquid and chiral orientated media, it has proved possible to measure the $(^2H/^1H)_i^{aniso}$ ratios for all ethylenic sites 9, 10, 12, and 13, and for the pro-*S* and pro-*R* positions of prochiral CH_2 sites 2, 3, 8, 14, and 15. Although the methylenic sites 4, 16, and 17 are also enantioresolved, the overlap of quadrupolar doublets precludes a precise determination of their respective $(^2H/^1H)_i^{aniso}$ ratios. Nevertheless, the data obtained from fully resolved sites can be used to evaluate, for the first time, the isotopic linkages *in vivo* between different hydrogen sources, including different isotopomers of glucose, and the different hydrogen positions in methyl linoleate.

Isotopic Linkage—The strength of the connections between each possible hydrogen source (water or glucose) and each site *i* of methyl linoleate resolved by ^2H NMR is described by the isotope redistribution coefficients, a_{im} for water and a_{ij}, which are obtained from Equations 3 and 4,

$$(^2H/^1H)_i^{aniso} = a_{ij}(^2H/^1H)_j + b \quad \text{(Eq. 3)}$$

$$(^2H/^1H)_i^{aniso} = a_{im}(^2H/^1H)_m + b \quad \text{(Eq. 4)}$$

which are the site-specific forms of Equation 1, expressing the $(^2H/^1H)_i^{aniso}$ ratios at site *i* of methyl linoleate in relation to the $(^2H/^1H)_j$ ratios of the slightly ^2H-enriched site *j* of glucose or acetate (Equation 3) used in cultures C–E or water (Equation 4) used in the culture B. In Equation 3, the slope a_{ij} reflects the contribution of labeled site *j* to the $(^2H/^1H)_i^{aniso}$ ratios of methyl linoleate, and the intercept *b* is the contribution of the other unlabeled sources present in the culture. Similarly, a_{im} in Equation 4 represents the input from water. The greater the value of $(^2H/^1H)_i^{aniso}$, the greater the contribution of $(^2H/^1H)_j$ or $(^2H/^1H)_m$ is to site *i*. To simplify the notation, the superscript "aniso" will be omitted hereafter. All the calculated a_{ij}, a_{im}, and *b* values at the CH_3 site (18), the CH_2 sites (2–8, 14–17), the enantio-resolved CH_2 sites (2, 3, 8, 14, 15), and the ethylenic sites CH (9, 10, 12, 13) are reported in Table 4. A similar analysis is not possible for cultures grown with [2-$^2H_3$]acetate because the $(^2H/^1H)_j$ ratio of acetate in the cells is not known, and thus the dilution factor cannot be calculated.

These linkages can then be analyzed in relation to the two different aspects of the biosynthetic pathway of linoleate, elongation and desaturation. The first consists of the formation of all CH_2 groups and the terminal CH_3, which come directly from its precursor stearyl-CoA. The second consists of the CH positions produced as a result of the action of desaturases (Fig. 2).

Isotopic Linkage at Methylenic Sites—As clearly illustrated in Fig. 3, a regular alternation is observed along the chain for a_{ij} values from CH_2 sites 2–18. This reflects the repetitive fashion by which consecutive two-carbon units are added from acetyl-CoA during the elongation of the fatty acid chain (1–3).

From the data in Table 4, mean values for the isotope redistribution coefficients, a_{im} and a_{ij}, and *b* can be calculated that represent the overall linkage to different types of hydrogen position, even CH_2 sites or odd CH_2 sites (Equations 5–10),

$$(^2H/^1H)_{CH_2}^{even} = 0.80(^2H/^1H)_m + 0.03 \quad \text{(Eq. 5)}$$

$$(^2H/^1H)_{CH_2}^{even} = 0.05(^2H/^1H)_{[6,6\text{-}^2H_2]gluc} + 111.0 \quad \text{(Eq. 6)}$$

$$(^2H/^1H)_{CH_2}^{even} = 0.006(^2H/^1H)_{[1\text{-}^2H]gluc} + 118.0 \quad \text{(Eq. 7)}$$

$$(^2H/^1H)_{CH_2}^{odd} = 0.37(^2H/^1H)_m + 76.2 \quad \text{(Eq. 8)}$$

$$(^2H/^1H)_{CH_2}^{odd} = 0.03(^2H/^1H)_{[6,6\text{-}^2H_2]gluc} + 119.4 \quad \text{(Eq. 9)}$$

$$(^2H/^1H)_{CH_2}^{odd} = 0.08(^2H/^1H)_{[1\text{-}^2H]gluc} + 109.1 \quad \text{(Eq. 10)}$$

From these equations, three general tendencies can be

TABLE 4

Calculated values of a_{ij} and *b* parameters for resolved sites of methyl linoleate isolated from ^{2}H-enriched cultures B–D

Culture	Site	2		3		4	5	6	7	8		9	10	11	12	13	14		15		16,17	18
		pro-*R*	pro-*S*	pro-*R*	pro-*S*	CH_2	CH_2	CH_2	CH_2	pro-*R*	pro-*S*	C=CH	C=CH	CH_2	C=CH	C=CH	pro-*R*	pro-*S*	pro-*R*	pro-*S*	$2CH_2$	CH_3
^2H_2O B	a_{ij}	0.77	0.89	0.33	0.19	0.76	0.35	0.90	0.34	0.58	0.69	0.15	0.92	0.36	0.78	0.30	0.81	0.90	0.79	0.34	0.59	0.59
	(±)[a]	(0.01)	(0.01)	(0.05)	(0.05)	(0.04)	(0.07)	(0.09)	(0.06)	(0.03)	(0.08)	(0.05)	(0.03)	(0.00)	(0.03)	(0.03)	(0.07)	(0.07)	(0.03)	(0.04)	(0.02)	(0.00)
	b	7.4	-6.8	85.0	62.6	-2.9[c]	69.0	-7.3[c]	65.1	21.1	1.5	37.8	2.6	57.0	-11.3[d]	61.9	10.5	-10.5	104.1	37.7	9.5	31.3
	(±)[b]	(0.9)	(0.9)	(7.5)	(7.5)	(6.3)	(10.6)	(13.7)	(8.9)	(4.4)	(11.5)	(8.0)	(4.3)	(0.1	(3.9)	(4.4)	(10.0)	(10.1)	(4.5)	(5.6)	(2.9)	(0.7)
[6,6-$^2H_2$]glucose C	a_{ij}	0.07	0.03	0.01	-0.01	0.05	0.02	0.08	0.03	0.05	-0.02	-0.03[d]	0.10	-0.01[c]	-0.02[d]	-0.03[d]	0.13	0.01	0.14	0.01	0.02	0.22
	(±)[a]	(0.02)	(0.02)	(0.02)	(0.02)	(0.03)	(0.00)	(0.00)	(0.02)	(0.02)	(0.01)	(0.02)	(0.01)	(0.00)	(0.02)	(0.01)	(0.02)	(0.01)	(0.03)	(0.03)	(0.04)	(0.01)
	b	111.3	120.5	132.6	92.3	102.8	117.8	115.3	111.9	106.4	106.1	64.5	89.8	111.8	108.4	111.9	112.9	122.0	201.1	86.1	93.8	86.9
	(±)[b]	(2.7)	(2.7)	(2.4)	(2.4)	(4.2)	(0.4)	(0.6)	(3.5)	(1.3)	(1.9)	(2.5)	(1.5)	(0.5)	(3.3)	(1.0)	(2.9)	(0.7)	(4.5)	(4.0)	(5.4)	(0.3)
[1-^{2}H]glucose D	a_{ij}	0.02	0.00	0.11	0.05	0.01	0.08	0.00	0.08	0.00	-0.01	0.03	0.06	0.06	-0.02[d]	0.05	0.02	0.00	0.18	0.06	0.05	0.05
	(±)[a]	(0.01)	(0.01)	(0.01)	(0.01)	(0.00)	(0.02)	(0.01)	(0.00)	(0.01)	(0.01)	(0.01)	(0.02)	(0.00)	(0.01)	(0.00)	(0.01)	(0.01)	(0.04)	(0.01)	(0.01)	(0.00)
	b	118.3	124.4	115.9	82.7	109.3	108.5	127.7	102.3	106.4	106.1	54.6	94.7	101.2	109.2	98.4	128.3	123.0	191.1	77.6	89.7	111.2
	(±)[b]	(1.7)	(1.7)	(2.3)	(2.3)	(0.7)	(3.3)	(1.2)	(0.7)	(1.3)	(1.9)	(2.1)	(2.7)	(0.5)	(1.0)	(0.4)	(1.6)	(1.7)	(6.4)	(1.2)	(0.7)	(0.1)

[a] Both higher and smaller a_{im} and a_{ij} values (a_h and a_s) are calculated from higher and smaller $(^2H/^1H)_i^{aniso}$ ratios (*i.e.* $(^2H/^1H)_i^{aniso} \pm$ S.D.). The value in parentheses corresponds to the accuracy of the a_{im} or a_{ij} parameter ($(\pm) = (a_h - a_s)/2$).

[b] The accuracy of the *b* parameter is calculated as described previously.

[c] Negative values should be considered equal to zero (precision within measurement).

[d] These double-bond sites result from desaturation steps during which one hydrogen atom is removed from the starting CH_2. Thus, linkage calculations are biased, which explains the presence of some negative values.

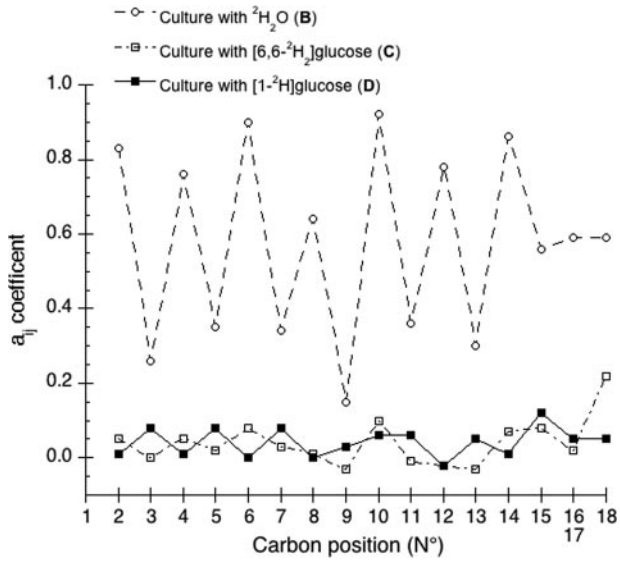

FIGURE 3. **Contribution of substrate (a_{ij} values) at different ^{2}H sites (2–18) along the methyl linoleate extracted from cultures B to D.** For the methylene sites 16 and 17, a mean value of a_{ij} is considered.

deduced. First, the hydrogens at both even and odd CH_2 sites are strongly linked to water but the former has a 2-fold greater link than the latter. Second, the C-1 of glucose contributes 10-fold more to the odd CH_2 sites than to the even. Third, both sites have a similar linkage to the C-6 position of glucose.

The analysis of the isotope redistribution coefficients can be further refined by considering separately the enantiomers at CH_2 that are enantio-resolved by using ^{2}H NMR in chiral oriented medium. Thus, the pro-*R* and pro-*S* positions at even CH_2 sites 2, 8, and 14 and odd CH_2 sites 3 and 15 can be resolved using Equations 11 and 12, respectively,

$$(^2H/^1H)_i^{pro\text{-}R} = k_{pro\text{-}R}(^2H/^1H)_j + c \quad \text{(Eq. 11)}$$

$$(^2H/^1H)_i^{pro\text{-}S} = k_{pro\text{-}S}(^2H/^1H)_j + c \quad \text{(Eq. 12)}$$

where the parameters $k_{pro\text{-}R}$ and $k_{pro\text{-}S}$ connect the pro-*R* and pro-*S* positions of CH_2 enantio-resolved sites, respectively, to the slightly enriched source of ^{2}H used in the cultures B–D.

At the even sites 2, 8, and 14, the $k_{pro\text{-}R}$, $k_{pro\text{-}S}$, and *c* values are similar, hence the mean values can be calculated (Equations 13–18),

$$(^2H/^1H)_{even\ CH_2}^{pro\text{-}S} = 0.83(^2H/^1H)_m - 5.3 \quad \text{(Eq. 13)}$$

$$(^2H/^1H)_{even\ CH_2}^{pro\text{-}S} = 0.01(^2H/^1H)_{[6,6\text{-}^2H_2]gluc} + 116.7 \quad \text{(Eq. 14)}$$

$$(^2H/^1H)_{even\ CH_2}^{pro\text{-}S} = 0.00(^2H/^1H)_{[1\text{-}^2H]gluc} + 117.8 \quad \text{(Eq. 15)}$$

$$(^2H/^1H)_{even\ CH_2}^{pro\text{-}R} = 0.72(^2H/^1H)_m + 13.0 \quad \text{(Eq. 16)}$$

$$(^2H/^1H)_{even\ CH_2}^{pro\text{-}R} = 0.08(^2H/^1H)_{[6,6\text{-}^2H]gluc} + 108.1 \quad \text{(Eq. 17)}$$

$$(^2H/^1H)_{even\ CH_2}^{pro\text{-}R} = 0.01(^2H/^1H)_{[1\text{-}^2H_2]gluc} + 117.7 \quad \text{(Eq. 18)}$$

These equations show that the strong linkage to water for the CH_2 sites (Equations 5 and 8) is not equivalent for the two hydrogen positions present, pro-*S* having a greater a_{im} than pro-*R*. Furthermore, the small overall linkage to the H-1 of glucose is now seen to be entirely with the pro-*R* position, which is also the position heavily favored for linkage to the H-6,6 of glucose. Thus, the enantio-resolution provides data that can potentially reflect the stereoselective addition and elimination of hydrogen atoms in the pro-*R* and pro-*S* positions.

In contrast to the situation with the even positions, the two odd enantio-resolved CH_2 sites 3 and 15 must be considered separately, because the enzymatic systems responsible for the elongation steps are different for chain formation up to C16 (FAS) and beyond (elongases). Thus, the data for site 3 (Table 4) relate to elongation (C16 → C18), whereas those for site 15 (Table 4) correspond to the chain-forming step C4 → C6.

From these isotope redistribution coefficients (Table 4), several features of the hydrogen isotopic linkage to these odd sites can be deduced and seen to be different. First, the contribution of medium water is 2–2.5-fold greater at site 15 than at site 3 for both pro-*R* and pro-*S* positions. Second, the H-1 of glucose also

contributes to both pro-*R* and pro-*S* positions of both sites 3 and 15. Again, it is notable that the contribution to the pro-*R* is 2–2.5-fold greater than to the pro-*S*. Third, the position H-6,6 of glucose contributes strongly to site 15 pro-*R* ($a_{ij} = 0.14$) but not at all to either site 15 pro-*S* or site 3 pro-*R*/*S*.

Isotopic Linkage at Ethylenic Sites—From the ^{2}H NMR spectra in chiral oriented media, it was also possible to measure all the $(^2H/^1H)_i^{aniso}$ ratios at ethylenic sites 9, 10, 12, and 13 (Table 3). This has not previously been achieved because of the lack of spectral resolution (compare supplemental Figs. SD1 and SD4). From the isotope redistribution coefficients thus obtained (Table 4), it can be seen that the even positions, 10 and 12, show a strong linkage to water, as seen for the even CH_2 sites, whereas the odd CH sites show a much lower value, more in the range of the odd CH_2 sites. However, for all four sites, the a_{ij} values linking the CH to H-1 and H-6,6 of glucose differ from those calculated for CH_2 sites, indicating a possible α-secondary KIE during the desaturation reaction.

DISCUSSION

The isotopic linkage in the different positions of methyl linoleate can be analyzed in relation to the two distinct parts of the biosynthetic pathway of linoleate, as indicated previously. The first consists of all CH_2 groups and the terminal CH_3, which are derived without modification from its precursor, stearoyl-CoA. The second consists of the CH groups, which are produced as a result of the action of Δ^9- and Δ^{12}-desaturases on the 9,10 sites of stearate and the 12,13 sites of oleate, respectively (Fig. 2). Based on the properties of the enzymes involved in the FAS and of the desaturases, it should be possible to interpret the observed $(^2H/^1H)_i^{aniso}$ values in terms of the known reaction characteristics. Hence, reaction characteristics for *F. lateritium* can be deduced.

Throughout the consecutive additions of two carbon units during chain growth within the FAS complex, steps that introduce or eliminate hydrogen during the creation of the CH_2 groups are both present. Thus, only the terminal methyl group retains all three hydrogen atoms derived from the CH_3 of acetyl-CoA. At even CH_2 sites (derived from the CH_3 of acetate), one hydrogen atom comes from acetyl-CoA (via malonyl-CoA) and the other is introduced from water by protonation by enoyl reductase (Fig. 1). However, the isotope redistribution coefficients from acetate will be diminished if post-malonate exchange with medium occurs (10, 11). At odd sites (derived from the C=O of acetate), the hydrogen atoms are introduced by the 3-oxoacyl-CoA reductase and the enoyl reductase, both linked to glucose via the NAD(P)H pool (Fig. 1). Thus, the isotope redistribution coefficients will not be affected by post-malonate exchange but could be influenced by exchange between NAD(P)H and water.

The 3-oxoacyl-CoA and the enoyl reductases transfer a hydride from (NAD(P)H), the stereoselectivity of transfer depends on the biological origin of the enzyme (34). Studies on fungal species other than yeast have demonstrated that protonation at even sites during enoyl reduction occurs at the *si*-face (35–37), as for *Saccharomyces cerevisiae* (38) and rat liver (39). Thus, in *F. lateritium,* pro-S_{even} and pro-R_{even} hydrogens should be introduced from water and water/acetate, respectively. However, no stereochemical information for fungi is available for hydride transfer at odd sites during enoyl reduction; for *S. cerevisiae*, stereoselectivity of the enoyl reductase has been completely described as 2*si*-3*si*. To what extent, then, can these origins and the relative stereochemistry be provided for *F. lateritium* from the present data?

Stereoselectivity of the FAS Complex and the Elongase in F. lateritium—As shown in Equations 5–10, the a_{ij} and a_{im} values calculated for CH_2 indicate that water, the H-1, and the H-6,6 of glucose all contribute hydrogen to CH_2 but to very different extents. Water has previously been identified as the main hydrogen source for the fatty acid chain in poultry, with high a_{ij} values at both even and odd CH_2 sites (18). In *F. lateritium*, however, two classes of CH_2 can clearly be distinguished on the basis of their mean values as follows: (i) the even CH_2 sites, with a mean $a_{im} = 0.80$ from water, $a_{ij} = 0.05$ from the H-6,6 of glucose, and $a_{ij} \approx 0.0$ from the H-1 of glucose; (ii) the odd CH_2 sites with a mean participation of $a_{im} = 0.37$ from water, $a_{ij} = 0.03$ from the H-6,6 of glucose, and $a_{ij} = 0.08$ from the H-1 of glucose. What then can be inferred from these links as to the relative influences of the origins of the hydrogen atoms?

Even Sites: Protonation during the Enoyl Reductase and Post-malonate Exchange—Equation 13 indicates that water is the unique donor of hydrogen at the pro-*S* position of even sites; the a_{im} is large (0.83), and the residue (b) is insignificant. This is confirmed when [^{2}H]glucose is used (Equations 14 and 15); the a_{ij} values are ≈ 0.0, whereas the residues are large. Thus, it can be deduced that the hydrogen atom at pro-*S* is introduced by *si*-face protonation of the *trans*-crotonyl-CoA intermediate, as observed in *S. cerevisiae* and in other fungi (35–37).

Consequently, as shown by the isotopic values measured for the methyl linoleate isolated from culture E grown in the presence of [2-$^2H_3$]acetate (Table 3), the hydrogen atom at pro-*R* comes from acetate. However, the degree of the post-malonate exchange that has occurred will influence the extent to which this hydrogen is acetate-derived or water-derived. This can be assessed by comparing the a_{ij} values observed (Table 4) in cultures B–D with that for the terminal methyl (site 18), because this site is directly derived from acetate.

Acetate is derived from glucose via both the glycolytic and pentose phosphate pathways, during which transfer from water occurs (see figures in Ref. 12). Thus, site 18 shows a significant transfer coefficient with water ($a_{im} = 0.59$) as well as with the H-6,6 ($a_{ij} = 0.22$) and H-1 of glucose ($a_{ij} = 0.05$). Because it is observed for the pro-*R* position of the even CH_2 groups that the participation of water clearly increases ($a_{ij} = 0.72$; see Equation 16), whereas those of the H-6,6 and H-1 of glucose strongly decrease (0.08; see Equation 17, and 0.01; see Equation 18, respectively), it can be concluded that a major exchange of hydrogen atoms from the CH_3 of acetate with the medium water during chain elaboration has occurred. Thus, post-malonate exchange (10, 11), taking place after the formation of malonyl-CoA, is found to strongly influence the hydrogen linkage in the pro-*R* position of even sites. This process has been described as very variable (11, 12, 39, 40).

Odd Sites, Recycling of Co-factors and Stereochemistry of Hydride Transfer during Reduction Steps—At odd CH_2 sites, both hydrogen atoms are introduced by two different reduction

steps, using NADH or NADPH as hydride donors. Although these will be primarily synthesized by the regeneration of $NAD(P)^+$ from glucose fermentation, other pathways active in aerobically grown *F. lateritium* might contribute. In particular, the reductive pentose phosphate pathway, in the course of which the H-1 and H-3 of glucose will be transferred to $NAD(P)^+$ (15, 17, 41).

The linkages obtained at odd CH_2 sites show that water is the main source of hydrogen ($a_{im} = 0.37$; see Equation 8), consistent with a substantial exchange of cofactor hydride with the medium, directly or via other water-labeled sources. It is noteworthy, however, that the participation of the H-6,6 and H-1 of glucose is significant ($a_{ij} = 0.03$; see Equation 9, and $a_{ij} = 0.08$; see Equation 10, respectively).

More detailed information on the reduction steps involved in the biosynthesis of the fatty acid chain in *F. lateritium* is obtained from the a_{ij} values calculated from the enantio-resolution of pro-*R* and pro-*S* positions at sites 3 and 15 (Table 4). It is evident that water is the main source of hydrogen for the pro-*R* and pro-*S* positions at both sites compared with glucose. However, two further points emerge from the values presented in Table 4 that require explanation as follows: (i) the dissimilar contributions of slightly enriched substrates to sites 3 and 15; (ii) the dissimilar contributions to the pro-*R* and pro-*S* positions for a given site (3 or 15), noting that a_{ij} for pro-*S* is always smaller than for the pro-*R* position.

Considering the observation i, a probable explanation lies in the nonequivalence of the enzymatic systems used by the cell for the elongation of the chain until C16 and then after C16. Not only are different enzymes involved, but these are not located in the same intracellular compartment (cytosol and endoplasmic reticulum in this case). Thus, the co-factor requirement and/or its recycling used for the reduction steps at sites 3 and 15 are unlikely to be the same. Consequently, the isotope ratio of NAD(P)H can be expected to differ at each location, leading to different $(^2H/^1H)$ ratios in the transferred hydride. A similar difference has been noted previously for the CH_2 at the position 3 in the biosynthesis of petroselinic acid (2).

In contrast, observation ii, that the a_{ij} values for all substrates tested were always smaller at the pro-*S* position than at the pro-*R*, requires an alternative explanation, because both reductions occur in the same cellular compartment. Rather, this difference is compatible with a different normal primary KIE occurring for hydride transfer from the co-factor to the fatty acid chain during one or both of the reduction steps. Clearly, hydride transfer to the pro-*S* position is subject to the stronger primary KIE, because a_{ij} for pro-*S* is always smaller than for pro-*R*. Furthermore, as the relationship of the $(^2H/^1H)_i^{aniso}$ ratios at the pro-*S* and pro-*R* positions is the same at sites 3 and 15, it can be inferred that their stereoselectivity is the same.

What cannot be deduced from the current data is which reduction step, the 3-oxoacyl reduction or the enoyl reduction, is submitted to the higher primary KIE. Currently, no information on the stereoselectivity of the enoyl reductase in fungi is available. This problem could be resolved by the ^2H NMR method used here, by comparing the ^2H distribution at sites 3 and 15 of methyl linoleate isolated from *F. lateritium* with the deuterium distribution of the same compound isolated from an organism for which the stereoselectivity of the enoyl reduction is already known, for example, the yeast *S. cerevisiae* (2*si*-3*si*).

Stereochemistry of the Desaturation Steps—The stereoselectivity of the removal of two vicinal hydrogen atoms from the acyl chain during desaturation to give a *cis* double bond seems to be conserved in all organisms (1–3). Previous studies (12–14) have shown that it is the pro-*R* hydrogens that are abstracted at positions 9,10 then 12,13 by the action of the Δ^9- and Δ^{12}-desaturases, respectively, leaving the pro-*S* hydrogen at all the ethylenic sites (Fig. 2). Hence, it is probable that the same stereoselectivity will be found in *F. lateritium*. The $(^2H/^1H)_{15}^{pro\text{-}S}$ ratios measured on methyl linoleate obtained from cultures A–E (Table 3) show strong coherence with the $(^2H/^1H)_9$ and $(^2H/^1H)_{13}$ ratios, but not with the $(^2H/^1H)_{15}^{pro\text{-}R}$ ratio, proving that the abstracted hydrogen atoms at odd sites 9 and 13 are also the pro-*R* in *F. lateritium*. At the even ethylenic positions 10 and 12, the $(^2H/^1H)_i^{aniso}$ ratios at pro-*R* and pro-*S* sites in cultures A–D are not sufficiently different to prove which hydrogen atom is abstracted (Table 3). However, when label was provided from [2-$^2H_3$]acetate (culture E), it is evident that the pro-*S* hydrogen atoms remained at these sites, because the even pro-*R* sites of methyl linoleate are highly enriched in these cultures (Table 3). Thus, as anticipated, all hydrogen atoms on the double bonds are shown to correspond to the pro-*S* hydrogen of the corresponding starting CH_2. This has not previously been determined for a filamentous fungus.

Secondary α-KIEs in the Desaturation Steps—Because the ^2H NMR in the chiral liquid crystal technique measures the $(^2H/^1H)_i$ ratios, it is possible to determine a secondary KIE on the carbon site α to the bond that is broken. A normal α-secondary KIE should decrease the $(^2H/^1H)_i$ ratio in the product at sites sensitive to this effect compared with sites that are not.

From Table 3 (cultures A–E), a comparison of the $(^2H/^1H)_9$ and $(^2H/^1H)_{13}$ ratios on one hand and of the $(^2H/^1H)_{10}$ and $(^2H/^1H)_{12}$ ratios on the other hand shows that the ratios at site 9 are, on average, lower than at site 13 (about −58 ppm) and that the $(^2H/^1H)_{12}$ ratios are, on average, lower than those at site 10 (about −44 ppm). These results are consistent with an α-secondary KIE occurring at site 9 but not at site 10 during the first desaturation, performed by the Δ^9-desaturase, and an α-secondary KIE at site 12 but not at site 13 during the second desaturation step, catalyzed by the Δ^{12}-desaturase. Such an α-secondary KIE has not previously been recorded for these desaturases. However, it is fully consistent with previous studies showing a primary KIE at site 9 but not at site 10 during the action of Δ^9-desaturase (42) and at site 12 but not at site 13 during the action of Δ^{12}-desaturase (43). Interestingly, the deuterium profile measured by ^2H NMR in chiral oriented media of methyl linoleate isolated from a plant (sunflower) shows similar $(^2H/^1H)_9$ and $(^2H/^1H)_{13}$ ratios, whereas the $(^2H/^1H)_{10}$ ratio was higher than the $(^2H/^1H)_{12}$ ratio (24). These measurements are in full agreement with the results found for the soluble plant Δ^9-desaturase, where no primary KIE at position 9 has been observed (44).

CONCLUSIONS

By exploiting the original and emerging technique of ^2H-{^1H} NMR in polypeptide chiral liquid crystals, it has proved possi-

ble, to measure the overall stereoselectivity that operates during the introduction of hydrogen atoms into the fatty acid chain, and the stereoselectivity of two desaturation steps *in vivo*. Stereoselectivity at prochiral centers has previously been examined in ethanol biosynthesis (16, 19), but such studies demanded the spectral resolution of the prochiral positions by chemical derivatization. The use of chiral aligned media both avoids this need and gives a direct and simple access to prochirality in complex molecules containing numerous prostereogenic centers, such as long chain fatty acids.

Whereas in ethanol (19) and lactate (17), the transfer coefficients observed between the fermented substrate (glucose) and certain hydrogen positions were very high, this was not the case here. Rather, the medium water is found to be the main donor of hydrogen atoms to all positions of the fatty acid chain in *F. lateritium*. Indeed, water is the exclusive donor at the pro-*S* positions of even CH_2 sites. Despite the fact that, theoretically, a strong linkage with the CH_3 of acetate and the pro-*R* positions of even sites should exist, a substantial proportion of hydrogen atoms is introduced from water, presumably by the phenomenon of post-malonate exchange. However, the extent of this is very much greater than the levels determined either *in vitro*, 18–36% (11), or *in vivo* (12–52%) from labeled acetate (12), indicating that this phenomenon alone does not entirely explain the hydrogen loss, which, as concluded by McInnes *et al.* (12), "is not related in a simple way to the type of fatty acid synthetase."

At odd sites, despite water also being the dominant source of hydrogen, it is possible to quantify a linkage with the non-exchangeable hydrogen atoms of glucose positions H-6,6 and H-1, which give rise to the CH_3 group of acetate. Hydrogens from both these positions are incorporated via acetyl-CoA, itself potentially derived from both glycolysis and the pentose phosphate pathway. It is seen that exogenous acetate, supplied as [2-$^2H_3$]acetate, enters the *in vivo* fatty acid biosynthesis pathway much more efficiently than glucose-derived acetate, probably explaining the lower yields of fatty acids obtained in our experiments compared with cultures grown on a mixture of glucose and acetate (26). However, it also confirms unambiguously the incorporation of hydrogen from the CH_3 of acetate to the pro-*R* position of the fatty acid chain, despite the post-malonate exchange.

The introduction of hydrogen atoms by the reduction step(s) into odd sites via NAD(P)H from position H-1 of glucose indicates a significant level of activity of the pentose phosphate pathway. This is supported by the much smaller incorporation seen from the H-6,6 of glucose, which cannot be by the same route but is likely to be via the Krebs cycle, a longer route that will lead to greater dilution.

In addition to analyzing the origin of the hydrogen atoms, it has proved possible to obtain data on the stereospecificity of the abstraction of hydrogen atoms during desaturation by Δ^9- and Δ^{12}-desaturases. It is shown that the hydrogen atoms abstracted at positions 9,10 and 12,13 are those at the pro-*R* positions, in agreement with previous findings for other organisms. Moreover, by comparing the ethylenic sites at pairs 9,13 and 10,12, α-secondary KIEs have been observed, as far as we are aware, for the first time for these desaturases.

A further outcome of this study is the demonstration of the great potential of using ^2H NMR in chiral weakly ordering media to obtain further information on the mechanism of enzymatic reactions, to elucidate enzyme stereoselectivity, and to identify precursors in relatively complex natural products. Work is now in hand to study other reactions of fatty acid chain modification, hydroxylation, epoxidation, and conjugation, which give rise to the diversity of the fatty acid family.

Acknowledgment—We thank Carol Wrigglesworth (Scientific English, Nantes) for critically reading the manuscript.

REFERENCES

1. Ohlrogge, J., and Browse, J. (1995) *Plant J.* **7,** 957–970
2. Kawaguchi, A., Iwamoto-Kihara, A., and Sato, N. (1999) *Comprehensive Natural Products Chemistry*, Vol. 1, pp. 23–59, Elsevier Science Publishing Co., Inc., New York
3. Rawlings, B. J. (1998) *Nat. Prod. Rep.* **15,** 275–308
4. Duan, J. R., Billault, I., Mabon, F., and Robins, R. (2002) *ChemBioChem* **3,** 752–759
5. Guiet, S., Robins, R. J., Lees, M., and Billault, I. (2003) *Phytochemistry* **64,** 227–233
6. Billault, I., Mantle, P. G., and Robins, R. J. (2004) *J. Am. Chem. Soc.* **126,** 3250–3256
7. Billault, I., Duan, J.-R., Guiet, S., and Robins, R. J. (2005) *J. Biol. Chem.* **280,** 17645–17651
8. Mizugaki, M., Kimura, C., Kondo, A., Kawaguchi, A., Okuda, S., and Yamanaka, H. (1984) *J. Biochem.* (*Tokyo*) **95,** 311–317
9. Marcinkeviciene, J., Jiang, W., Kopcho, L. M., Locke, G., Luo, Y., and Copeland, R. A. (2001) *Arch. Biochem. Biophys.* **390,** 101–108
10. Sedgwick, B., Cornforth, J., French, S., Gray, R., Kelstrup, E., and Willadsen, P. (1977) *Eur. J. Biochem.* **75,** 481–495
11. Sedgwick, B., and Cornforth, J. (1977) *Eur. J. Biochem.* **75,** 465–479
12. McInnes, A., Walker, J., and Wright, J. (1983) *Tetrahedron* **39,** 3515–3522
13. Schroepfer, G., and Bloch, K. (1965) *J. Biol. Chem.* **240,** 54–63
14. Morris, L. J. (1970) *Biochem. J.* **118,** 681–693
15. Zhang, B.-L., Yunianta, and Martin, M. (1995) *J. Biol. Chem.* **270,** 16023–16029
16. Pionnier, S., Robins, R., and Zhang, B.-L. (2003) *J. Agric. Food Chem.* **51,** 2076–2082
17. Roger, O., Lavigne, R., Mahmoud, M., Buisson, C., Onno, B., Zhang, B. L., and Robins, R. J. (2004) *J. Biol. Chem.* **279,** 24923–24928
18. Zhang, B. L., Pionnier, S., and Buddrus, S. (2006) *Eur. J. Lipid Sci. Technol.* **108,** 125–133
19. Robins, R. J., Pétavy, F., Nemmaoui, Y., Ayadi, F., Silvestre, V., and Zhang, B. L. (2008) *J. Biol. Chem.* **283,** 9704–9712
20. Schmidt, H.-L., Werner, R., and Eisenreich, W. (2003) *Phytochem. Rev.* **2,** 61–85
21. Robins, R., Billault, I., Duan, J.-R., Guiet, S., Pionnier, S., and Zhang, B.-L. (2003) *Phytochem. Rev.* **2,** 87–102
22. Duan, J.-R. (2002) *Distribution Naturelle du Deutérium d'Acides Gras Isolés d'Huiles, Végétales, Etude Quantitative par RMN.* Ph.D. thesis, University of Nantes, Nantes, France
23. Aroulanda, C., Merlet, D., Courtieu, J., and Lesot, P. (2001) *J. Am. Chem. Soc.* **123,** 12059–12066
24. Lesot, P., Baillif, V., and Billault, I. (2008) *Anal. Chem.* **80,** 2963–2972
25. Baillif, V., Robins, D. J., Billault, I., and Lesot, P. (2006) *J. Am. Chem. Soc.* **128,** 11180–11187
26. Gorbik, L., Pidoplichko, G., and Loiko, Z. (1980) *Mikrobiol. Zh.* (*Kiev*) **42,** 191–196
27. Shanklin, J., and Cahoon, E. B. (1998) *Annu. Rev. Plant Physiol.* **49,** 611–641
28. Zhang, B.-L., Billault, I., Li, X.-B., Mabon, F., Remaud, G., and Martin, M. (2002) *J. Agric. Food Chem.* **50,** 1574–1580
29. Sarfati, M., Lesot, P., Merlet, D., and Courtieu, J. (2000) *Chem. Commun.*

21, 2069–2081
30. Lesot, P., Sarfati, M., and Courtieu, J. (2003) *Chem. Eur. J.* **9,** 1724–1745
31. Lafon, O., Lesot, P., Merlet, D., and Courtieu, J. (2004) *J. Magn. Reson.* **171,** 135–142
32. Martin, M., and Martin, G. (1990) in *NMR Basic Principles and Progress* (Diehl, P., Fluck, E., Günther, H., Kosfeld, R., and Seelig, J., eds) pp. 1–63, Springer-Verlag, Berlin
33. Lesot, P., Aroulanda, C., and Billault, I. (2004) *Anal. Chem.* **76,** 2827–2835
34. O'Hagan, D. (1992) *The Polyketide Metabolites* pp. 19–43, Ellis Horwood, UK
35. Reese, P. B., Rawlings, B. J., Ramer, S. E., and Vederas, J. C. (1988) *J. Am. Chem. Soc.* **110,** 316–318
36. Townsend, C. A., and Brobst, S. W. (1988) *J. Am. Chem. Soc.* **110,** 318–319
37. Rawlings, B. J., Reese, P. B., Ramer, S. E., and Vederas, J. C. (1989) *J. Am. Chem. Soc.* **111,** 3382–3390
38. Sedgwick, B., and Morris, C. (1980) *J.C.S. Chem. Comm.* **3,** 96–97
39. Saito, K., Kawaguchi, A., Seyama, Y., Yamakawa, T., and Okuda, S. (1981) *J. Biochem.* (*Tokyo*) **90,** 1697–1704
40. Saito, K., Kawaguchi, A., Nozoe, S., Seyama, Y., and Okuda, S. (1982) *Biochem. Biophys. Res. Commun.* **108,** 995–1001
41. Zhang, B. L., and Pionnier, S. (2003) *Chem. Eur. J.* **9,** 3604–3610
42. Buist, P., and Behrouzian, B. (1996) *J. Am. Chem. Soc.* **118,** 6295–6296
43. Buist, P., and Behrouzian, B. (1998) *J. Am. Chem. Soc.* **120,** 871–876
44. Behrouzian, B., Buist, P., and Shanklin, J. (2001) *Chem. Comm.* **5,** 401–402